A first chronology for the East GReenland Ice–core Project (EGRIP) over the Holocene and last glacial termination

Seyedhamidreza Mojtabavi[1,2], Frank Wilhelms[1,2], Eliza Cook[3], Siwan Davies[4], Giulia Sinnl[3], Mathias Skov Jensen[3], Dorthe Dahl-Jensen[3], Anders Svensson[3], Bo Vinther[3], Sepp Kipfstuhl[1,3], Gwydion Jones[4], Nanna B. Karlsson[1,5], Sergio Henrique Faria[6,7,8], Vasileios Gkinis[3], Helle Kjær[3], Tobias Erhardt[9], Sarah M. P. Berben[10], Kerim H. Nisancioglu[10,11], Iben Koldtoft[3], and Sune Olander Rasmussen[3]

[1]Alfred–Wegener–Institut Helmholtz–Zentrum für Polar– und Meeresforschung, Bremerhaven, Germany
[2]Department of Crystallography, Geoscience Centre, University of Göttingen, 37073 Göttingen, Germany
[3]Physics of Ice, Climate and Earth, Niels Bohr Institute, University of Copenhagen, Denmark
[4]Department of Geography, College of Science, Swansea University, Swansea, Wales, UK
[5]Geological Survey of Denmark and Greenland, Copenhagen, Denmark
[6]Basque Centre for Climate Change (BC3), 48940 Leioa, Spain
[7]Nagaoka University of Technology, 940-2188 Nagaoka, Japan
[8]IKERBASQUE, Basque Foundation for Science, 48011 Bilbao, Spain
[9]Climate and Environmental Physics, Physics Institute and Oeschger Center for Climate Change Research, University of Bern, Sidlerstrasse 5, 3012 Bern, Switzerland
[10]Department of Earth Science, University of Bergen, Bjerknes Centre for Climate Research, Allégaten 41, 5007, Bergen, Norway
[11]Centre for Earth Evolution and Dynamics, University of Oslo, Oslo, Norway

Correspondence: Seyedhamidreza Mojtabavi (Seyedhamidreza.Mojtabavi@awi.de)

Abstract.

This paper provides the first chronology for the deep ice core from the East GReenland Ice-core Project (EGRIP) over the Holocene and late last glacial period. We rely mainly on volcanic events and common patterns of peaks in dielectric profiling (DEP), electrical conductivity measurements (ECM) and tephra records for the synchronization between the EGRIP, NEEM

5 and NGRIP ice cores in Greenland. We transfer the annual-layer-counted Greenland Ice Core Chronology 2005 (GICC05) timescale from the NGRIP core to the EGRIP ice core by means of 373 match points. The NEEM ice core is only used for supporting match-point identification. We name our EGRIP time scale GICC05-EGRIP-1. Over the uppermost 1383.84 m, we establish a depth–age relationship dating back to 14,965 a b2k (years before the year 2000 CE). Tephra horizons provide an independent validation of our match points. In addition, we compare the ratio of annual layer thicknesses between ice cores

10 in-between the match points to assess our results in view of the different ice-flow patterns and accumulation regimes of the different periods and geographical regions. This initial timescale is the basis of interpretation and refinement of the presently derived EGRIP high-resolution data sets of chemical impurities.

1 Introduction

The dating of an ice core establishes the depth–age relationship to construct a chronology of past climatic conditions from the
15 measured proxy parameters, reflect immediate past atmospheric conditions and biogeochemical events. The climatic studies of
the core will focus on high-resolution climate records of greenhouse gasses, water isotopes, physical properties and impurities
through the last 25,000 years covering the onset of the present interglacial, the climatic optimum 8,000 years ago and the
industrial period of the past two hundred years.

In relation to the ice sheet, the depth–age relation is needed to interpret and understand the climatic evolution and the
20 behaviour of individual ice streams. This is a particular focus of the East GReenland Ice-core Project (EGRIP). The drill site
has been chosen close to the onset of the North East Greenland Ice Stream (NEGIS) (see Fig. 1), which is the largest ice stream
of the Greenland ice sheet (Joughin et al., 2010, 2018). The idea behind the EGRIP project is to study dynamics of the ice flow
in the NEGIS. In addition to the objectives related to ice dynamics, obtaining climate records going at least half way through
the glacial period is expected.

25 The annual-layer-counted Greenland Ice Core Chronology 2005 (GICC05) is derived from measurements of stable water
isotopes in the DYE–3, GRIP and NGRIP (see Fig. 1) ice cores for the period back to 7.9 ka b2k (Vinther et al., 2006) and high-
resolution measurements of chemical impurities, conductivity of the ice, and visual stratigraphy from the GRIP and NGRIP
ice cores for the period between 7.9 ka and 14.7 ka b2k (Rasmussen et al., 2006). For the period from 14.7 to 42 ka b2k, the
dating of the cores is based on annual layer counting in the visual stratigraphy, the electrical conductivity profiles, and a set
30 of chemical impurities data (Andersen et al., 2006). The time scale is compared to time scales of other climate archives like
marine cores at tie points (Svensson et al., 2006). For the NGRIP core, the GICC05 time scale has been extended even further
back into the glacial back to 60 ka b2k by annual layer counting (Svensson et al., 2008) and extended by ice-flow modelling
(Wolff et al., 2010). The GICC05modelext timescale was transferred from NGRIP to the NEEM ice core by matching 787
match points of mainly volcanic origin identified in the electrical conductivity measurement (ECM) and dielectric profiling
35 (DEP) records and – where available – verified by tephra horizons (Rasmussen et al., 2013). The GICC05modelext was also
applied to the central Greenland GRIP and GISP2 cores by chemo-stratigraphic matching of more than 900 marker points and
verification with 24 tephra horizons (Seierstad et al., 2014).

The upper ∼ 1400 m of the EGRIP core has been profiled by means of ECM and DEP in the field during the 2017, 2018 and
2019 field seasons. The objective of this study is to establish an initial chronology for the EGRIP ice core over the Holocene
40 and last glacial termination by applying the GICC05 timescale to the EGRIP core. We rely on volcanic events: the common
patterns of peaks in the DEP and ECM records, and identified tephra horizons for the synchronization between the EGRIP ice
core, the North Greenland Eemian (NEEM) ice core, and the NGRIP1 and NGRIP2 cores from the North Greenland Ice Core
Project. The NEEM ice core is used for supporting match-point identification, while the GICC05 ages are transferred from
NGRIP to EGRIP.
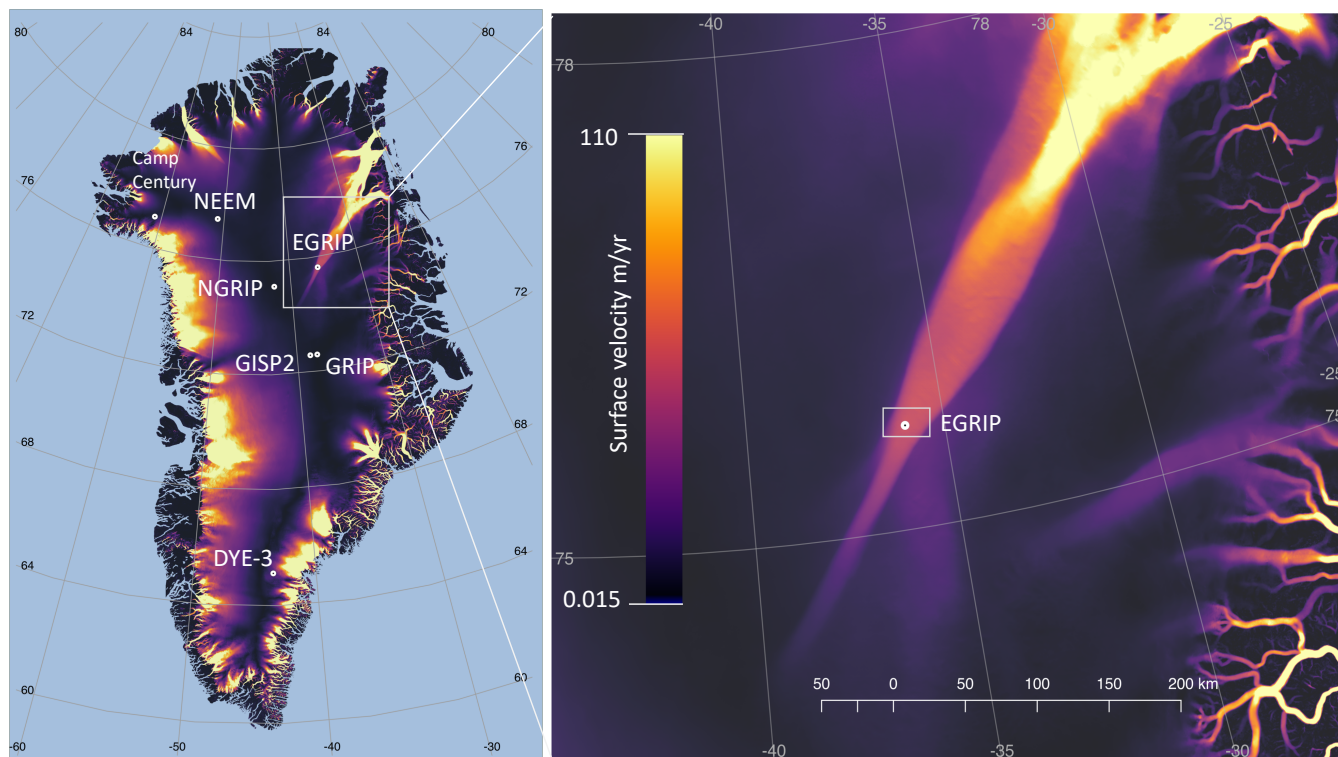
Figure 1. Locations of deep ice-core drill sites: EGRIP, NEEM, NGRIP, GRIP, GISP2, DYE–3, and Camp Century in Greenland, and close-up of the EGRIP drill site inside the North East Greenland Ice Stream (NEGIS). Colours show surface flow velocities from satellite data (Joughin et al., 2018).

2 Data and methods

2.1 Ice-core data sets over the Holocene and last glacial termination

2.1.1 EGRIP

Here, we processed and analysed new DEP, ECM and tephra measurements in the upper ~ 1400 m of the EGRIP ice core. At the start of drilling in 2016, the drilling site was located at $75^{\circ}38'$ N and $35^{\circ}60'$ W (see Fig. 1). The average annual accumulation rate is around 0.11 m for the period 1607–2011 as reconstructed based on a firn core close to main EGRIP drill site (Vallelonga et al., 2014). The camp currently moves around 51 m to the North-Northeast each year (Dahl-Jensen et al., 2019). Fig 2 shows an overview of the sections of ice for each core that we used in this study.

2.1.2 NGRIP

The GICC05 is a Greenland annual-layer-counted chronology based on data from several cores reaching about 60.2 ka back
in time. For the older parts (Wolff et al., 2010) the NGRIP ss09sea06bm model time scale, shifted to younger ages by 705
years, has been spliced onto the end of the GICC05 timescale, thereby forming the so-called GICC05modelext chronology,
which was also applied to the NEEM core. The synchronization used ECM data supplemented by DEP signals for matching the
deeper part. To fully exploit the potential of DEP records for matching, we processed unpublished DEP data from the NGRIP1
core for the upper part (down to 1298 m), and we used the NGRIP2 (below 1298 m) that was published with the NGRIP ECM
data in Rasmussen et al. (2013). The NGRIP1 and NGRIP2 cores have a depth offset of around 0.43 m between corresponding
events in the overlapping section (Rasmussen et al., 2013).

2.1.3 NEEM

The firn core NEEM–2008–S1 refers to the access hole of the NEEM main core, drilled during the 2008 field season to a depth
of 103 m. We used only ECM data for the matching of the upper 100 m, as DEP analyses were not made. Below this depth,
both DEP and ECM were used (Rasmussen et al., 2013). The shallow and deep cores overlap, forming a continuous record.
To check the quality of the ECM data on the NEEM–2018–S1 core, we compared the data to high electrolytical meltwater
conductivity measurements (Gfeller et al., 2014) and find good correspondence between peaks in the two datasets.
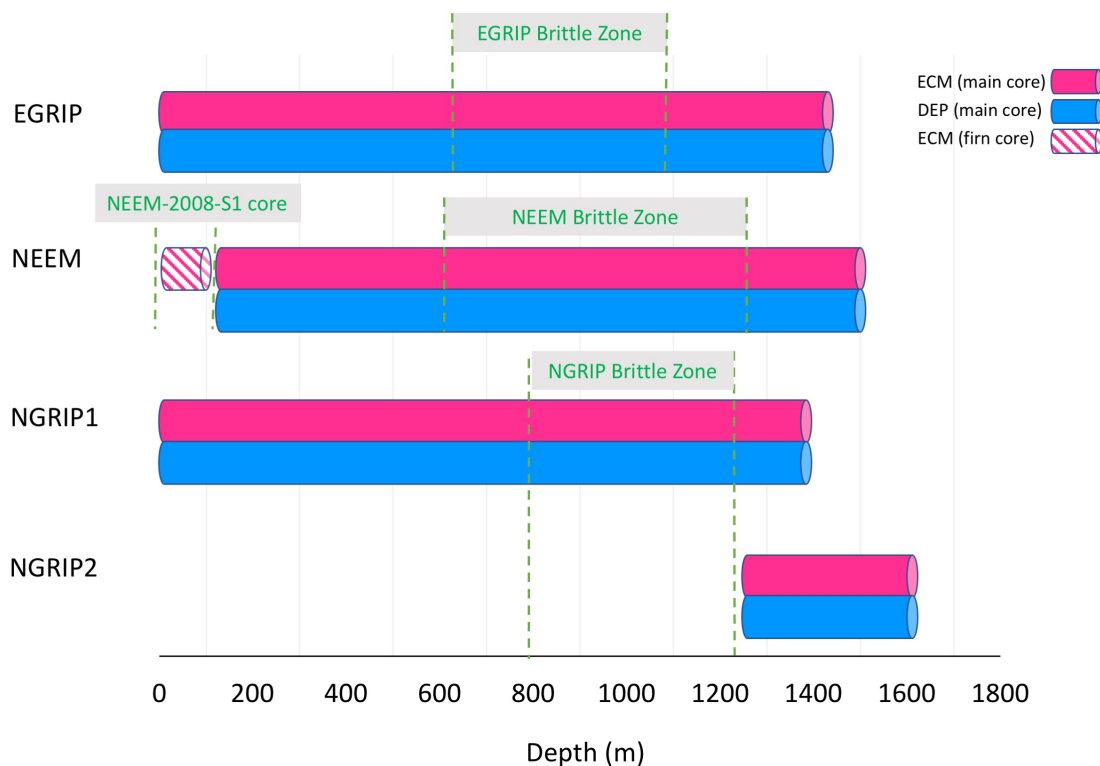
Figure 2. Overview of dielectrical profiling (DEP) and electrical conductivity measurements (ECM) that we used for the synchronization between ice cores over the Holocene and late last glacial periods.

2.2 Field measurements and data processing

2.2.1 Dielectric profiling (DEP)

70 Dielectric Profiling (DEP) has been introduced as a system for rapid dielectric profiling of ice cores shortly after drilling (Moore and Paren, 1987). The recorded permittivity and conductivity of ice and firn are determined by their respective densities and conductivities (Wilhelms, 2005). The conductivity is related mainly to acidity, salt and ammonia concentrations of ice cores (Moore et al., 1992, 1994). The dielectric stratigraphy of the EGRIP, NEEM and NGRIP cores were recorded directly during the field seasons with the DEP device described by Wilhelms et al. (1998). DEP is the first measurement within the processing

75 line directly on site. A few minutes before scanning, the core is moved from the core buffer to the DEP table. Further along the processing line the ice core is split into the different aliquots. For all three ice cores, DEP measurements were performed in 1.65 m long sections.

For the calibration of the DEP device, free-air measurements without ice was recorded frequently, usually at least twice daily before processing started and finished, respectively. The slight capacitance and conductance variation on the order of less than 4 fF and 500 pS along the DEP device is due to the unavoidable deformation of the cables when moving the scanning electrode along the device. Additionally, a few nS of residual conductance may remain even after performing the correction routines of the LCR meter (inductance L, capacitance C, resistance R) bridge. This offset, introduced by the changing stray admittance due to the varying cable geometry during the measurement, is additive and treated by subtracting the course of free-air measurements along the DEP device when processing the data.

For the processing of the NGRIP cores, reproducibility was ensured by laying the cables out to move freely in the same way for all measurements in between two recorded free-air measurements. This was improved for the NEEM and EGRIP processing by placing the cables into cable channels, that enforce repeatable deformation.

The free-air measurement scans the empty capacitor along the DEP device, where the conductance of the air as the capacitor's dielectric vanishes. Thus, the conductance of a scanned ice core is straightforwardly corrected by subtraction of the conductance of the free air measurement. In contrast, the recorded free air capacitance is composed from the capacitance of the empty device and the fraction to be corrected due to cable stray and possibly further small residual offsets in the order of few 1 fF after correction. The computation of the fraction to correct for cable stray therefore requires the knowledge of the DEP device's actual free air capacitance. The free air capacitance is also a factor in the computation of the ice's material properties from the capacitor's capacitance and conductance readings, when filled with the ice core sample as a dielectric.

All cores were scanned with the DEP device as described in (Wilhelms, 1996; Wilhelms et al., 1998). The theoretical value of 63.4 fF and the measured free air capacitance for a precisely adjusted DEP bench coincide within 2 fF. The small difference might well be due to mechanical tolerances like the electrode length in the range of a few tenths of a mm. However, for a slightly differently adjusted device (one with slightly more clearance to the core, for example), the deviation from the ideal value of the free air capacitance might be a few fF higher. Precise permittivity and resultingly precise free air capacitance values mainly make a difference when computing the wave propagation speed of radar waves while modelling synthetic radargrams (Eisen et al., 2006). As the datasets will also be used for this purpose later (Mojtabavi et al., 2019), we determined the free air capacitance by averaging the measured capacitance over deep core sections and dividing with the expected permittivity of ice of 3.18 ± 0.1 which computes the free air capacitance with 3% relative error, which is only about 2 fF absolute error for the free air capacitance.

For the NGRIP and the NEEM cores, we had no other means to precisely determine the free air capacitance as outlined above. For the EGRIP core processing, the DEP bench was upgraded with a rack to mount tubes of different diameters concentric to the DEP electrodes and record the capacitance along the DEP device. The tube in the electric field increases the capacitance of the arrangement and Wilhelms (2000) derives the theory to calculate the effective permittivity of the setup. For the calibration, tubes with radius in approximately 10 mm increments between 0–70mm represented effective permittivities between 1 to 4 (Figure 3). The result is a calibration curve which holds for the calculation of a consistent free air capacitance for the correction of DEP measurement of the EGRIP core. The free air capacitance is the proportionality factor of the measured capacitance and the effective permittivity, i.e. the slope of the graph in Figure 3.
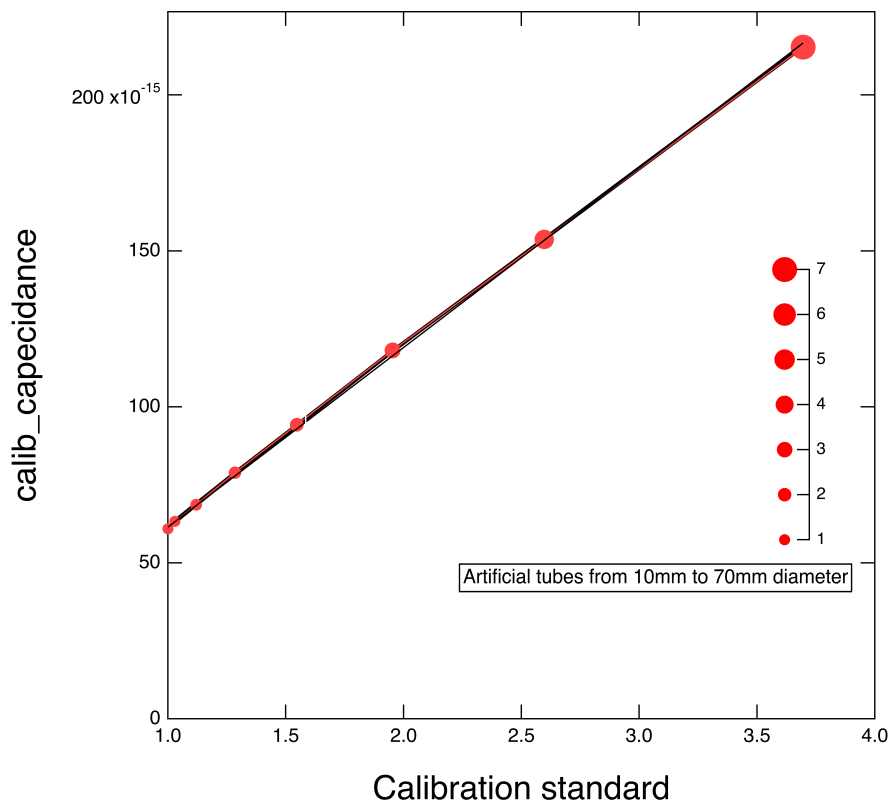
Figure 3. Calibration curve of the measurements with artificial tubes and free-air measurement for DEP device

Due to the drilling procedure and properties of the ice, ice cores can exhibit breaks, broken-off slices or may in some instances (especially in the brittle zone) be fragmented. The missing pieces and free surfaces with possibly high conductivity

115 have the potential to introduce artefacts into the DEP record. These are clearly identifiable in the permittivity record by dropping spikes. For the validation of the data, any drop below a certain threshold (cf. the red line in Figure 4) identifies a spike to be rejected, where the segment to be rejected is extended to about the average of the permittivity record. The procedure is described in Rasmussen et al. (2013). This automated validation is much faster and comparably good as the standard way of noting deficient core sections in a field protocol, accessing each noted area on a single case basis and validating the data. It even

120 does not depend on the quality of the protocol, as it might have a wrong note about depth of the ice cores breaks. In this way, it not only validates the permittivity record but also the conductivity record. The NEEM, the EGRIP and the NGRIP records were validated in this way.

At this point, the DEP data is not yet corrected for the temperature variation in the science trench or core-buffer, however this correction does not affect the use of conductivity peaks for synchronization purposes between ice cores.
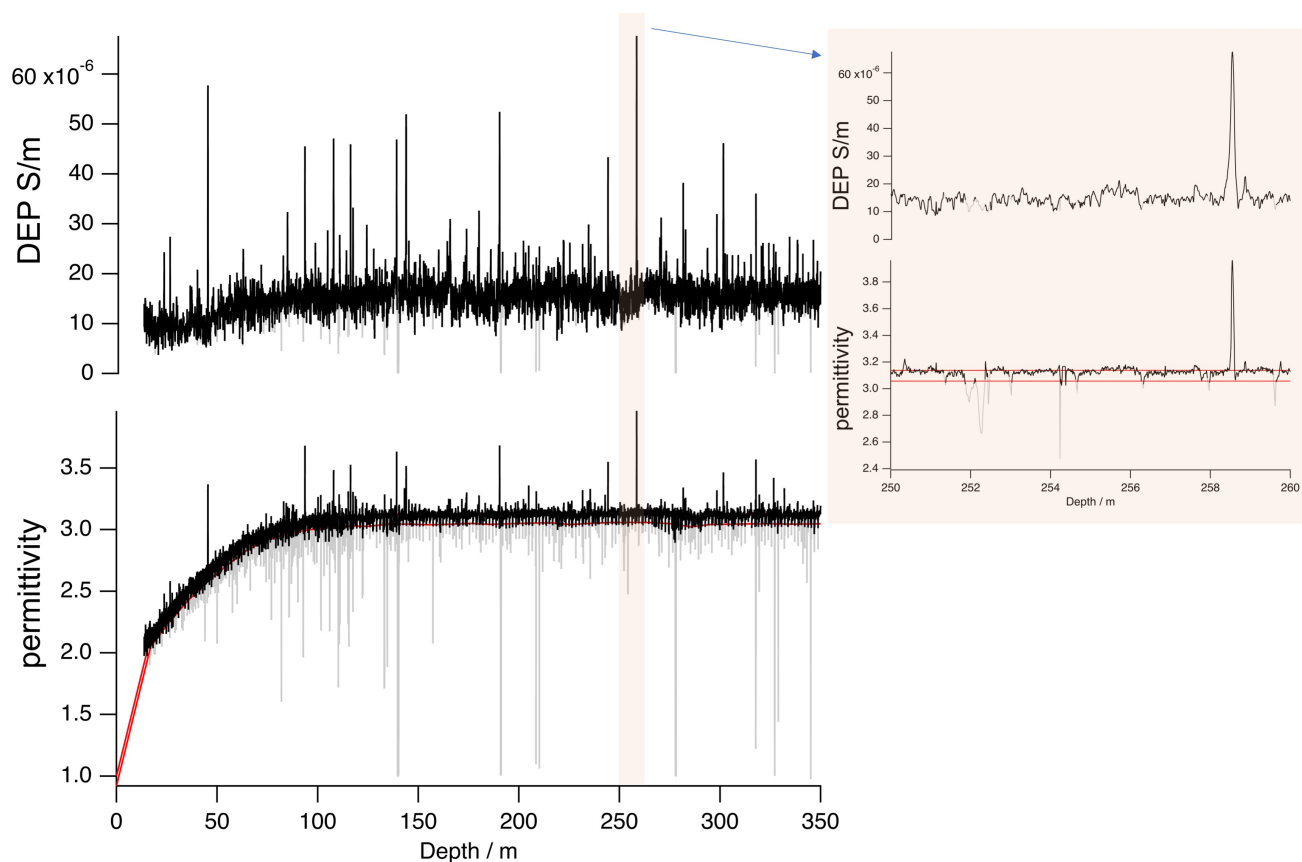
Figure 4. Example of DEP data processing (removing core breaks from the raw data). The permittivity measurement is in grey and after processing in black (bottom). The permittivity drops below the red line and shows bad quality of ice-core sections. As seen above (top), corresponding conductivity before processing data (grey) and after processing data (black). The insert shows the details for a short section (250–260 m).

125   When processing the EGRIP core, over a certain period the operators did not reset the starting position of the scanning electrode of the DEP device, which is clearly identifiable in the records. It resulted in measuring too early before the starting position of the core (blue arrows in Figure 5), then recording the correct length increment, but resultingly missing the corresponding length at the end of the core section. The respective core section has to be shifted accordingly. The reconstructed DEP record was then compared and validated against the ECM record to assign the correct depths. The section about 1285–

130   1385m was corrected. Furthermore, we relied more heavily on the ECM record than on the DEP record in sections with known problems. Figure 5 illustrates the corrections in the interval 1299.10–1302.05 m, where a 35 cm data gap between two scanned sections cannot be reconstructed as it was not recorded due to the wrong positioning of the electrode.
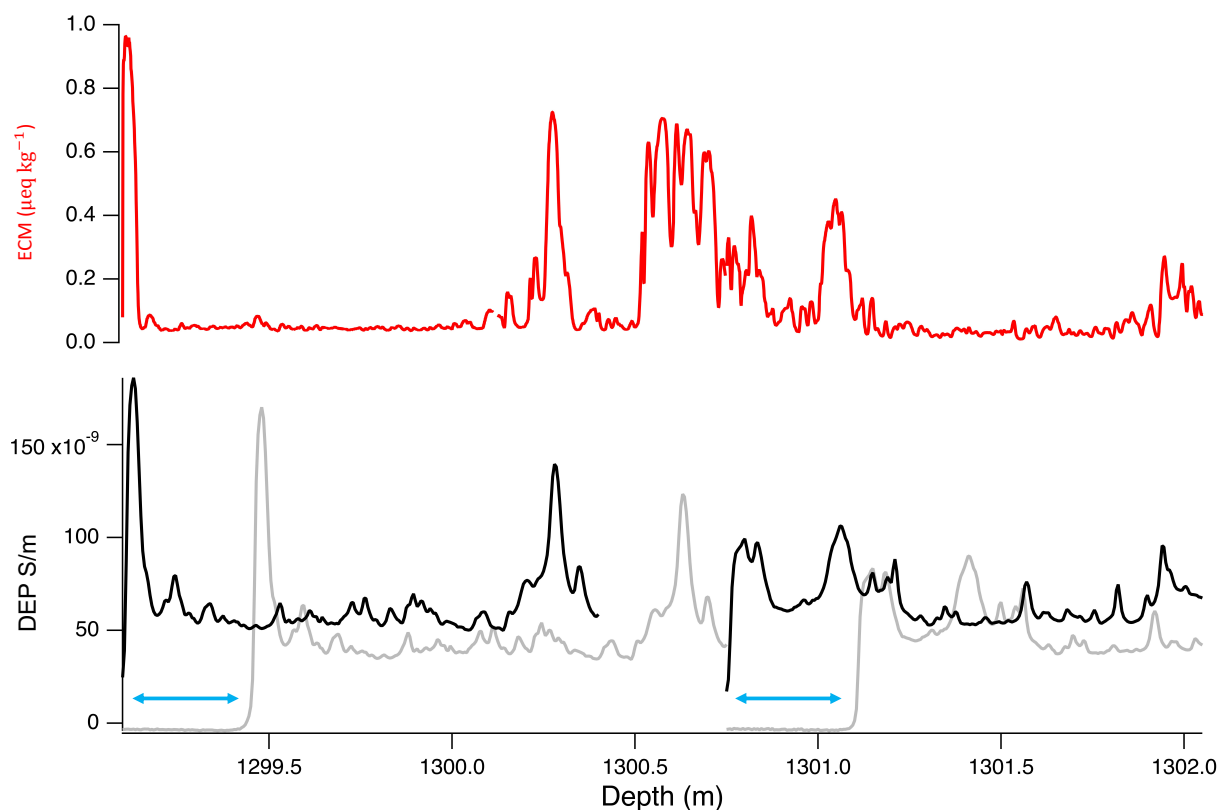
Figure 5. Example of the DEP data gap length and relative precision of ECM vs DEP depth assignment. The DEP measurement with a wrong depth in grey and after shifting depth in black. There is a gap of 35 cm (1300.4–1300.75 m) between two DEP measurements. Blue arrows show the early measurements before the starting position of the core. Corresponding ECM data in red.

2.2.2 Electrical conductivity measurements (ECM)

For the EGRIP core, we recorded ECM profiles with the technique described by Hammer (1980) directly in the field. The ECM
135 signal is related to acidity concentrations of ice cores, even with high concentrations of neutral salt (Moore et al., 1992). NGRIP (Dahl-Jensen et al., 2002) and NEEM (Rasmussen et al., 2013) were measured using identical equipment during the respective processing campaigns in the field. For each measurement, the hand-held ECM instrument was moved along the depth axis of the ice-core sections' microtomed surface (three-bag sections, around 1.65 m). In order to calibrate ECM data, as described in Rasmussen et al. (2013), the ice temperature was measured for each run. In addition, to ensure the ECM quality, we repeated
140 our measurement at least twice for each core section and checked the profiles for the best quality of the measurements. Also, the core breaks were registered by reading out the positions of the hand-held ECM instrument at the respective break position after the measurement of each core section. During the processing, the recorded breaks were used to trim off artefacts and produce the used ECM data set. Data from each day were calibrated using independent measurements of the physical dimensions of

the ECM measurement setup. The first and last few millimetres of recorded data are affected by the proximity to the end of the

145 core and were removed. Areas with dips in the signal around logged core breaks were also muted during processing. The depth

scale of the ECM profile was assigned based on the recorded movement of the electrodes interpolated between the logged

top and bottom depth of individual ice-core sections. To investigate the quality of the depth assignment, a bag mark position

analysis was carried out on the section below the brittle zone in EGRIP, ∼1160–1760 m. Only ice core sections with a core

length of 1.65 m were included in the analysis. Each 1.65 m section contains the equivalent of three 0.55 m bags, and the

150 position of the bag marks separating the first and second bags and the second and third bags, respectively, are known. During

ECM measurements, these bag marks are logged (just as the break marks), but not used for the processing. After processing of

the ECM signal, the position of logged bag marks were interpolated onto the same depth scale as the processed ECM signal,

making it possible to compare the true depth of these marks to their depths in the processed data. The distance in depth between

logged and expected positions of individual bag marks were calculated for all sections included in the analysis. It was found

155 that the depth assignment of the bag marks were almost always accurate within 20 mm, with mean distance $\mu = 8.3$ mm and

standard deviation $\sigma = 7.9$ mm. The ECM current, i (in μA), was converted to ice acidity (in μequiv. $H^+ kg^{-1}$) by using

the relationship $[H^+] = 0.045 \times i^{1.73}$, as suggested by Hammer (1980). Even though conversion from current to acidity and

calibration curves have been shown to be ice-core dependent, the matching and synchronization of the ice cores is independent

of the absolute values of the calibrated ECM signal as it relies on recognition of similar patterns and peaks in the acidity records

160 (Rasmussen et al., 2013).

The quality of the processed data were checked by comparing independently processed ECM data by three investigators. No

major disagreements were found when comparing, and one set of data was agreed on for further use in matching.

2.2.3 Tephra horizons

Tephra sampling of the EGRIP core in the field was continuous to maximize the identification of volcanic ash deposits, par-

165 ticularly invisible deposits that are comprised of low concentrations and/or small grain sizes, known as cryptotephra (Davies,

2015). A strip of ice was cut from the outer curved edge of each 55 cm ice core section and subsampled at a 11 cm resolution,

providing approximately 30 ml of meltwater per sample. Of these, sections of ice that contained either significant peaks in the

DEP and ECM or visible layers were separated and prioritized for screening, whereby centrifuged samples were evaporated

onto microscope slides and mounted in epoxy resin to enable scanning by light microscopy, as described by Cook et al. (2018).

170 Electron probe microanalysis (EPMA) by wavelength dispersive spectrometry (WDS) was performed to determine the major

element compositions of individual grains in each deposit (Hayward, 2012) and EPMA measurements were performed using a

Cameca SX100 electron probe microanalyzer at the Tephrochronology Analytical Unit, University of Edinburgh. This system

has five wave dispersive (WD) spectrometers and was calibrated daily using internal calibration standards as described by Hay-

ward (2012). Operating conditions were optimized for analysis of small cryptotephra grains (<20 μm diameter) and EGRIP

175 samples were analysed with either a 5 or 3 μm beam diameter. Analysis of secondary standards was performed to identify

instrumental drift. The geochemical composition of each layer was compared to deposits in NGRIP and positive matches were

used to establish tie-points between cores shown in Table 1. Major element biplots (Figure 6) show graphical correlations

Table 1. Geochemical matches between EGRIP and NGRIP were supported by the similarity coefficient test (SC) of Borchardt et al. (1972) and statistical distance (D2) test of Perkins et al. (1995, 1998). Here we provide SC and D2 values for major elements (normalized to 100%) where 5 major elements (with >%1wt) were used for SC calculations for sample pairs with rhyolitic composition and 7 elements were used for sample pairs with basaltic composition. Values >0.95 suggest products are from the same volcanic source. For D2, seven major elements were used for the comparisons (with >0.01 %wt). The value for testing the statistical distance values at the 99% confidence interval is 18.48 (seven degrees of freedom).

EGRIP Bag	Depth range	NGRIP /GRIP match	SC	D^2
177	96.91–97.02 m	NGRIP 142.61–142.71 m	0.985	1.65
1627	894.41–894.52 m	NGRIP 1163.65–1163.80 m	0.977	4.88
2094	1151.59–1151.70 m	NGRIP 1408.88–1408.89 m (Mortensen et al., 2005)	0.965	5.945

for each NGRIP–EGRIP tephra match point, and these are supported by similarity coefficient (Borchardt et al., 1972) and statistical distance (D^2) (Perkins et al., 1995, 1998) tests.
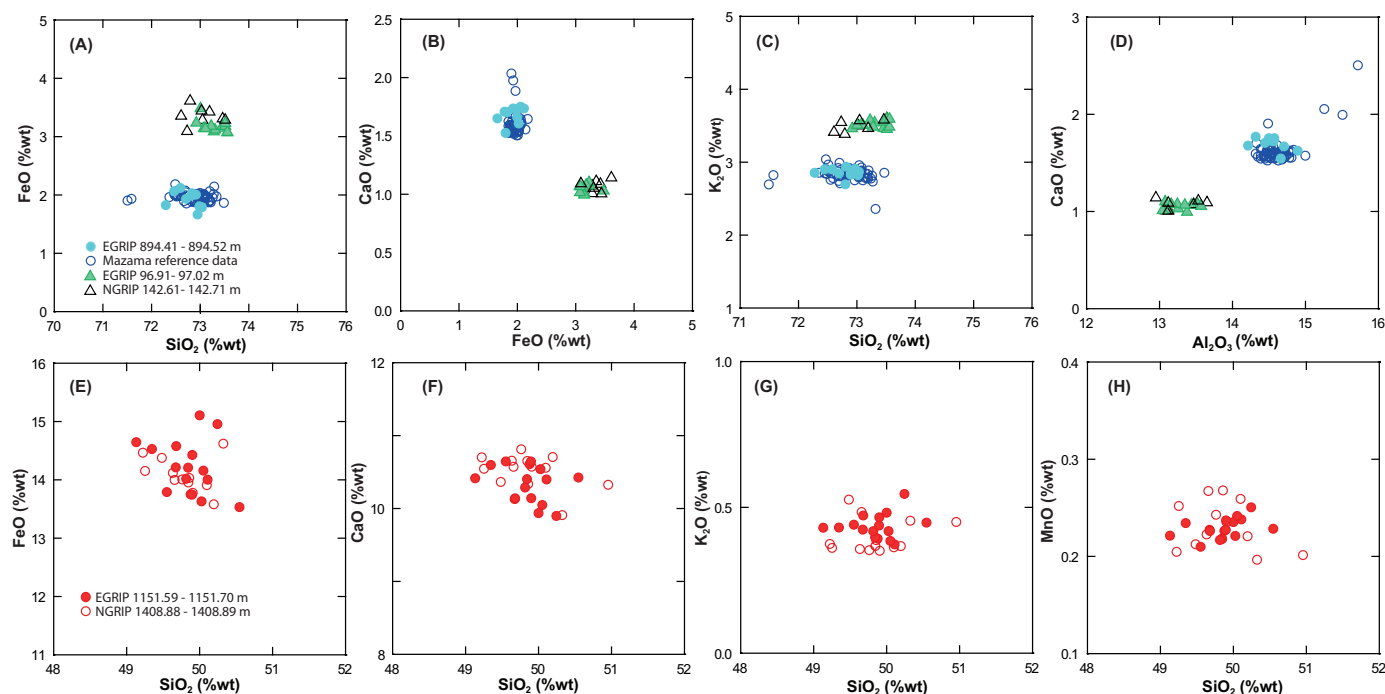
Figure 6. Element–element biplots showing geochemical matches between EGRIP and NGRIP samples with the exception of EGRIP 894.41–894.52 m, which is shown here with Mazama data from Jensen et al. (2019). Geochemical data are normalised to 100% (anhydrous basis) and analyses with totals below 94 %wt were excluded.

2.3 Synchronization of dielectric profiling and electrical conductivity measurement records of the ice cores

Patterns in the DEP and ECM data were matched between ice cores separately and independently, mainly based on the volcanic events and also non-volcanic events. All sections were matched between NGRIP, NEEM and EGRIP synchronously, meaning all three ice cores had been combined on the screen. To finalize match points, common patterns were selected and confirmed with all four investigators for each dataset. In order to find match points between ice cores, we used the Matchmaker tool (Rasmussen et al., 2013) that can track offset match points during matching phases when aligning and evaluating data. The most sensitive test to validate match points is to plot the depth of common match points for two ice cores, $\Delta D(i) = D(i) - D(i+1)$, $\Delta d(i) = d(i) - d(i+1)$ and the ratio $r = \Delta D(i)/\Delta d(i)$ of annual layer thicknesses, where D and d are the depths of the common volcanic or non-volcanic events in two different cores. We expected only significant change in the smoothness of the (depth vs. depth) curve of match points with different climate conditions and climate transitions in ice-core sections (Rasmussen et al., 2006, 2013; Seierstad et al., 2014; Winski et al., 2019). Furthermore, these tests are provided to investigate our results

based on glaciologically realistic outcomes, for example, the different ice-flow pattern and accumulation regimes at the different sites in Greenland (Rasmussen et al., 2013).

2.4 Transfer of the GICC05 timescale to the EGRIP ice core

We transferred the GICC05 time scale to the EGRIP ice core by interpolation between match points for each ice core bag (i.e., 0.55 m depth intervals). First, we assumed a slight annual layer thickness variation between the ice cores based on the reasonable assumption of accumulation variability and from the smoothness curve of the depth of common match points (see section 2.3). Therefore, the EGRIP depths were transferred to NGRIP depths by linear interpolation between match points. By this approach, the ages are obtained from the GICC05 (depth, age) relation based on NGRIP depths (Rasmussen et al., 2013). The GICC05 includes the so-called Maximum Counting Error (MCE) in which the uncertain layers are counted as 1/2 ± 1/2 yr (Rasmussen et al., 2013). We used linear and cubic spline interpolations to estimate uncertainty and precision of the interpolated timescale between match points.

3 Results and discussion

3.1 Synchronization of the EGRIP, NEEM and NGRIP cores

A total of 249 match points between the EGRIP, NEEM and NGRIP1 ice cores and 124 match points between EGRIP, NEEM and NGRIP2 (total of 373 match points) with an additional three tephra horizons were identified. Figure 7 shows an example section of ECM/DEP matched between ice cores. The total match points between ice cores are shown on Figure 8. In the process of combining match points from all investigators, some match points were removed due to differences in the peak shapes between DEP and ECM data or when there were too many match points very close to each other. There are fewer match points in the interval 600–1100 m due to the brittle zone in sections in NEEM and NGRIP1. The sections of alkaline ice associated with stadial conditions in EGRIP where the ECM and DEP do not follow each other closely due to high dust levels neutralizing the acidity of the ice (Ruth et al., 2003; Rasmussen et al., 2013).
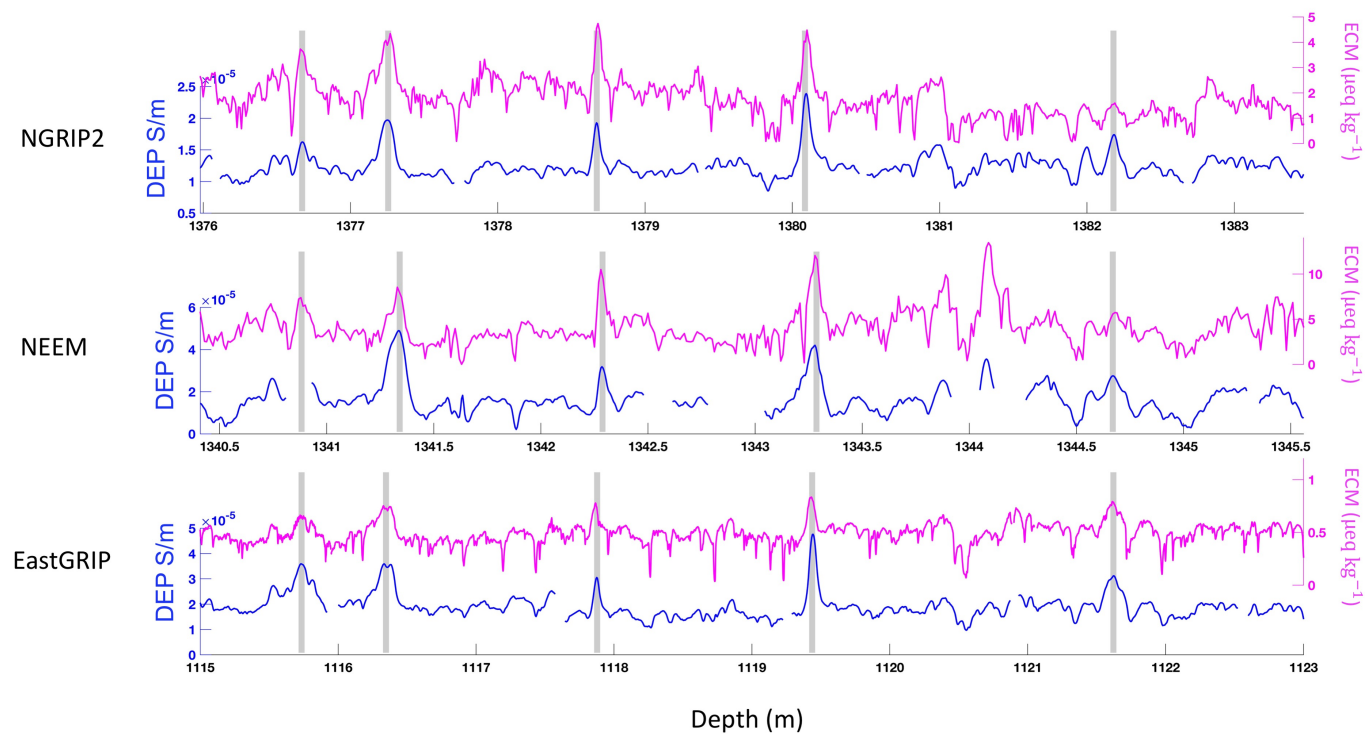
Figure 7. Example of ECM and DEP data matching between the NGRIP2 (top), NEEM (middle) and EGRIP (bottom) cores. The match points are marked by grey bands.
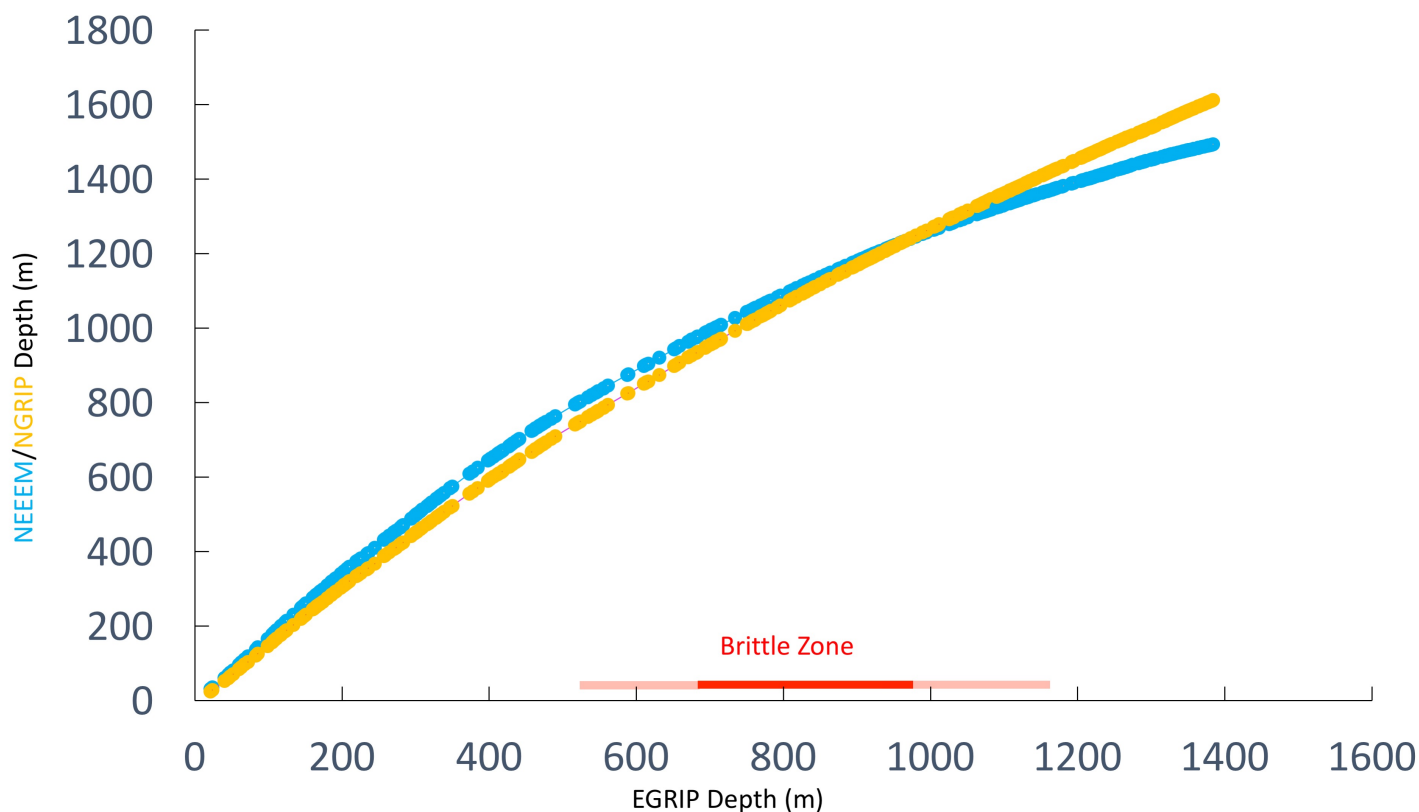
Figure 8. Match points between EGRIP, NEEM (blue) and NGRIP (yellow) ice cores based on the DEP and ECM data sets.

3.2 Tephra horizons identified for the chronology

Three tephra horizons have been located in EGRIP (Table 1). The locations of these horizons were consistent with the DEP and ECM based synchronization. The tephra horizons thus provide an independent validation for our match points. In addition, ongoing tephra investigations will likely provide additional points for synchronization between ice cores in intervals without DEP and ECM match points.

3.3 GICC05-EGRIP-1

As described in section 2.4, the timescale was transferred from the NGRIP GICC05 (depth, age) to the EGRIP ice core based on 373 match points. The relationship between depth and age for EGRIP over the Holocene and early last glacial periods is named GICC05-EGRIP-1 and the average annual layer thickness between the match points is presented (Figure 9).

We synchronized the records of the EGRIP, NEEM and NGRIP ice cores back to 14.96 ka b2k which corresponds to 1383.84 m, 1493.29 m and 1611.98 m depth, respectively. Note that we assumed that the ratio of annual layer thicknesses is constant between the match points of EGRIP and NGRIP. The depths in NGRIP of the match points were interpolated to the EGRIP,

and then the ages are obtained from the NGRIP GICC05 (depth, age) relation. We used different methods of interpolation
(linear vs. cubic spline interpolation) between match points to estimate the uncertainty of these different interpolations. The
difference in result is around 0–2 yr for most sections. Therefore, obtaining the age directly from the EGRIP (depth, age) with
the assumption of constant annual layer thicknesses between match points and interpolating ages between match points provide
different results and that is an unrealistic pattern for the accumulation rates (Rasmussen et al., 2013). The smooth relationship
between the depths of the EGRIP and the NEEM respectively NGRIP depths match points is due to the smooth change of
relative annual layer thicknesses. Figure 10 shows that EGRIP has thinner annual layers than both NEEM and NGRIP ice cores
when the upper part of the three records are compared. This is because lower accumulation leads to thinner annual layers.
Due to increasing upstream accumulation rates and less thinning at EGRIP compared to NGRIP and NEEM, annual layers in
EGRIP eventually gets thicker with depth compared to annual layers in the NEEM and NGRIP ice cores. In EGRIP, the flow
regime is different, compared to an ice core close to the ice divide like NEEM and NGRIP. By pure coincidence the combined
effects of increasing upstream accumulation and flow-induced thinning give roughly constant annual layer thicknesses back to
$\sim$ 8000 yr in EGRIP. (Figure 9). The accumulation upstream is supposedly higher than at the EGRIP site and thus as older
ice comes from upstream and had more time to thin the annual layers become equal thickness in the EGRIP ice core. In most
ice cores in the proximity of ice divides, the annual layer thickness drops almost linearly with depth for the Holocene part of
the record. As NGRIP and NEEM layers get thinner in this way (Rasmussen et al., 2013), EGRIP layers start to get thinner
but remains nearly constant in thickness. Below an EGRIP depth of around 700 m, annual layers in EGRIP are thicker than
the layers from the same period in the NEEM core, and similarly below 1000 m, EGRIP annual layers are thicker than those
in NGRIP(Figure 10). There are some gaps in the EGRIP ice-core record due to the brittle zone. However, we believe the
smoothness of the depth vs. depth plot in Figure 8 and the annual layer thickness ratio in Figure 10 shows a good agreement
for our time scale based on the match points. As described in section 2.4, the uncertainty of the GICC05-EGRIP-1 timescale
is based on the maximum counting error (MCE) of the GICC05 timescale. When more annual layer data become available it
can provide more details for the EGRIP ice core and the time scale can be improved by layer counting.
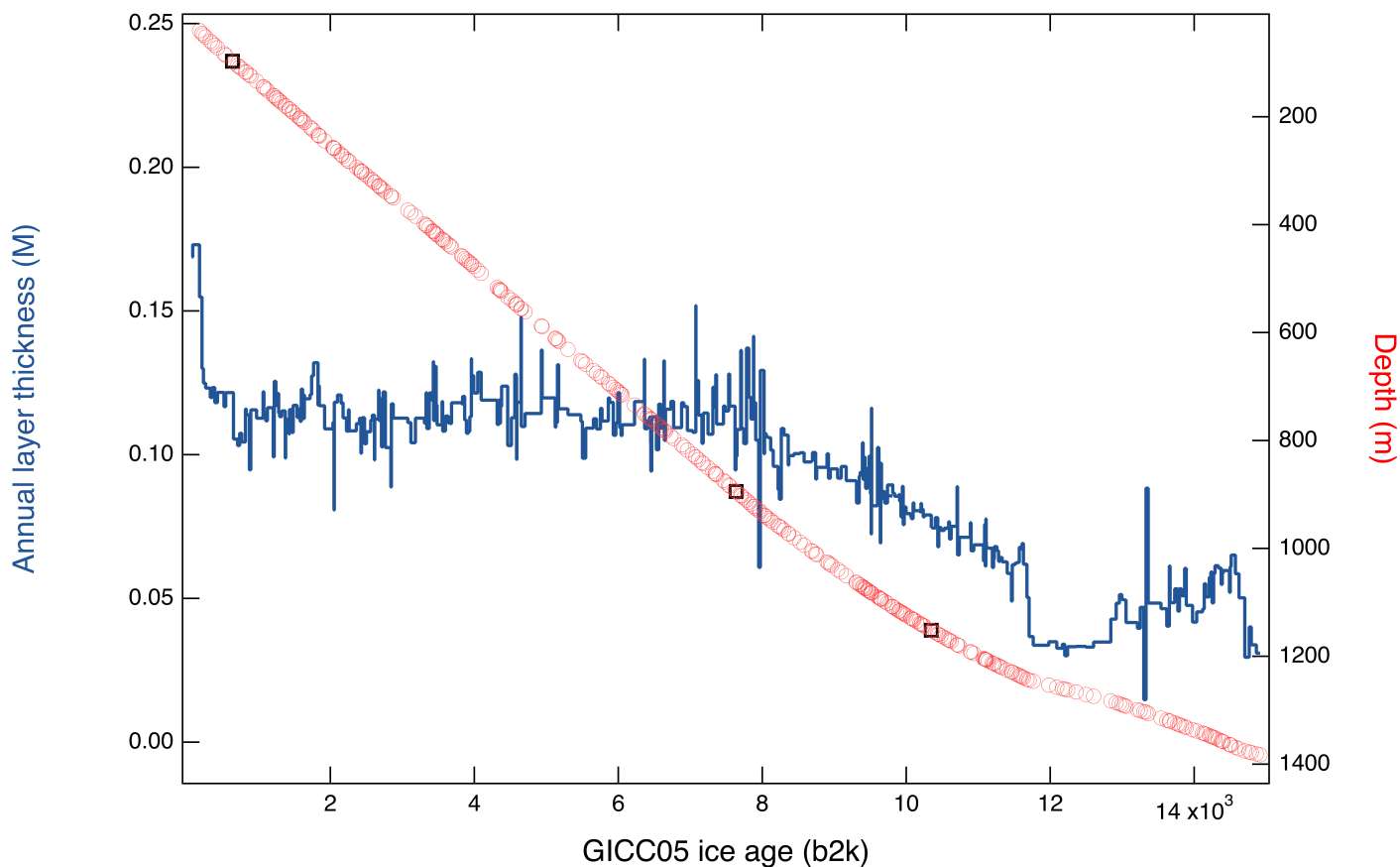
Figure 9. EGRIP annual layer thicknesses (dark blue line, left y-axis) between the match points. The EGRIP depth–age relationship (right y-axis) with match points (red dots) and the tephra horizons (black squares).
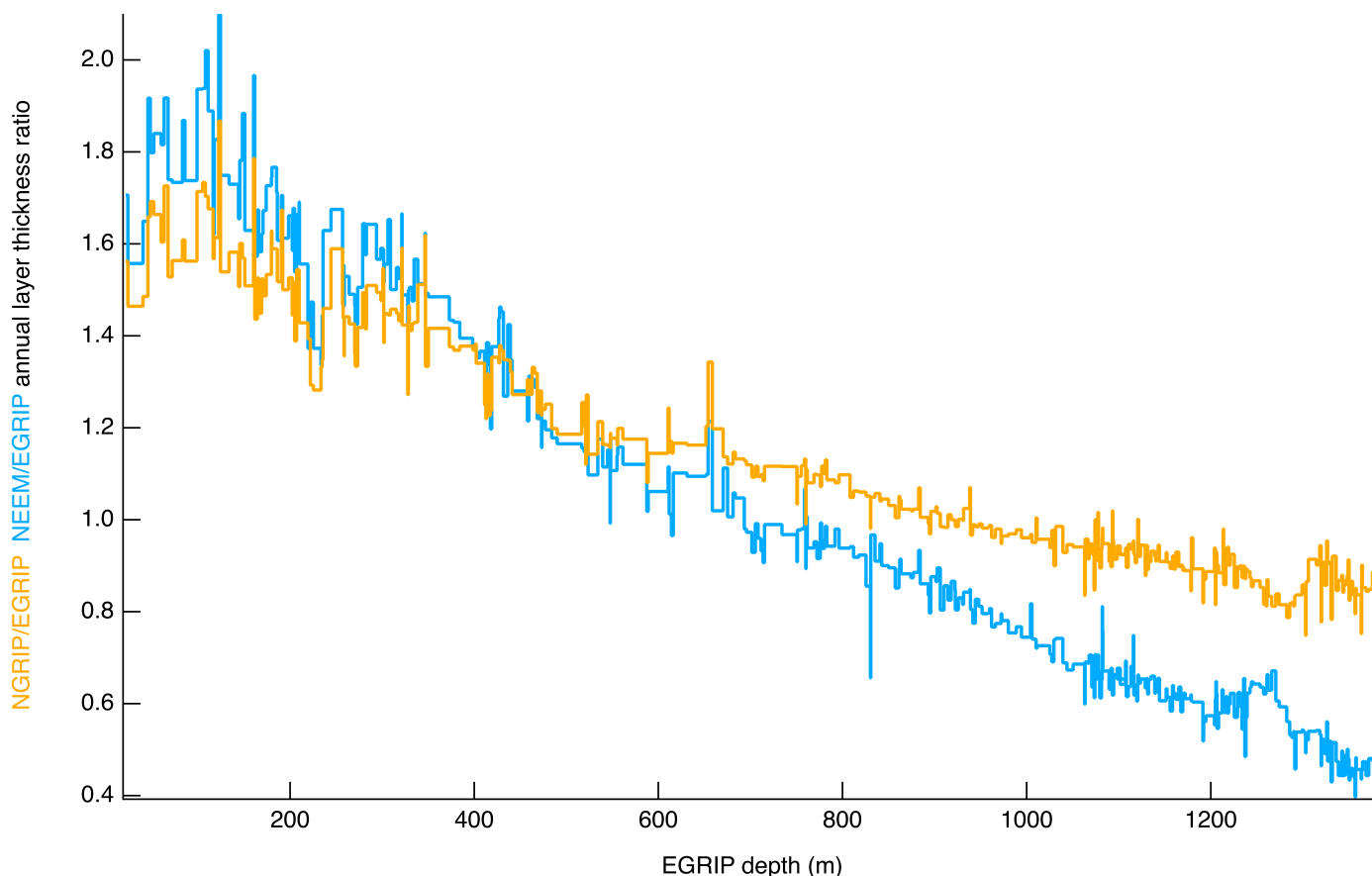
Figure 10. The NGRIP/EGRIP (orange) and NEEM/EGRIP (blue) annual-layer thickness ratio (left axis) between the match points.

4   Conclusions

We have established the initial chronology for the EGRIP deep ice core in Greenland which encompasses the Holocene and late glacial periods. We have established the depth–age relation for the upper ∼ 1400 m of the core back to approximately 14.96

250   ka b2k based on the GICC05 time scale and labelled it GICC05-EGRIP-1. After field measurements and processing of the ice-core data, we rely on the DEP and ECM records for the synchronization, using 373 match points between EGRIP, NEEM and NGRIP ice cores. The identification of tephra match points between EGRIP and NGRIP cores provide an independent tool for validating this synchronization. The ratio of annual layer thicknesses between ice cores has been used as a tool to evaluate our match points based on the different ice flow patterns and accumulation regimes in the different regions. This first timescale

255   can help to interpret, design sampling strategies and improve understanding of forthcoming EGRIP data sets.

5 Supplementary data

With the final version of this paper we will publish the following data sets at www.pangaea.de and www.iceandclimate.dk/data:
– ECM data from EGRIP in 1 mm resolution (down to 1383.84 m). – DEP data from EGRIP (down to 1383.84 m), NGRIP1 (down to 1372 m) in 5 mm resolution. – The match points (including the tephra horizons depths) used for the time scale transfer. – The EGRIP (depth, age) relation in 0.55 m ("bag") resolution.

Author contributions. Original draft preparation by SM with major contributions from FW, SOR, EC, MSJ; matching by SM, FW, SOR, GS, MSJ; DEP data processing by SM, FW; ECM data processing by SOR, GS, MSJ; tephra data processing by EC, SD, GJ; DEP measurements in the field by SM, SK, NAB, SHF, VG, HK; ECM measurements in the field by SM, SOR, HK, TE, KN, SMPB, SHF, IK; preperation, set-up and testing of DEP system by SM, FW; preperation, set-up and testing of ECM system by BV, DDJ, SOR; tephra selection and sampling in the field by EC, SM, SD, SMPB; All authors contributed to improving the final paper.

Acknowledgements. We thank all people involved in logistics, drilling and ice-core processing in the field. EGRIP is directed and organized by the Center of Ice and Climate at the Niels Bohr Institute. It is supported by funding agencies and institutions in Denmark (A. P. Møller Foundation, University of Copenhagen), USA (US National Science Foundation, Office of Polar Programs), Germany (Alfred Wegener Institute, Helmholtz Centre for Polar and Marine Research), Japan (National Institute of Polar Research and Artic Challenge for Sustainability), Norway (University of Bergen and Bergen Research Foundation), Switzerland (Swiss National Science Foundation), France (French Polar Institute Paul–Emile Victor, Institute for Geosciences and Environmental research) and China (Chinese Academy of Sciences and Beijing Normal University). Sune Olander Rasmussen and Giulia Sinnl gratefully acknowledge the Carlsberg Foundation for support to the project ChronoClimate. Sergio Henrique Faria acknowledges support from the project iMechPro (RTI2018–100696–B–I00) from the Spanish Ministry of Science, Innovation, and Universities and from the Ramón y Cajal grant RYC–2012–12167 of the Spanish Ministry of Economy, Industry and Competitiveness.

References

Andersen, K. K., Svensson, A., Johnsen, S. J., Rasmussen, S. O., Bigler, M., Röthlisberger, R., Ruth, U., Siggaard-Andersen, M.-L., Steffensen, J. P., Dahl-Jensen, D., Vinther, B. M., and Clausen, H. B.: The Greenland Ice Core Chronology 2005, 15–42ka. Part 1: constructing the time scale, Quaternary Science Reviews, 25, 3246 – 3257, https://doi.org/https://doi.org/10.1016/j.quascirev.2006.08.002, http://www.sciencedirect.com/science/article/pii/S0277379106002587, 2006.

Borchardt, G. A., Aruscavage, . J., and Millard, H. T.: Correlation of the Bishop Ash, a Pleistocene marker bed, using instrumental neutron activation analysis, Journal of Sedimentary Research, 42, 301–306, https://doi.org/10.1306/74D72527-2B21-11D7-8648000102C1865D, 1972.

Cook, E., Davies, S. M., Guðmundsdóttir, E. R., Abbott, P. M., and Pearce, N. J. G.: First identification and characterization of Borrobol-type tephra in the Greenland ice cores: new deposits and improved age estimates, Journal of Quaternary Science, 33, 212–224, https://doi.org/10.1002/jqs.3016, https://onlinelibrary.wiley.com/doi/abs/10.1002/jqs.3016, 2018.

Dahl-Jensen, D., Gundestrup, N. S., Miller, H., Watanabe, O., Johnsen, S. J., Steffensen, J. P., Clausen, H. B., Svensson, A., and Larsen, L. B.: The NorthGRIP deep drilling programme, Annals of Glaciology, 35, 1–4, https://doi.org/10.3189/172756402781817275, 2002.

Dahl-Jensen, D., Kirk, M., Koldtoft, I., Popp, T., and P, S. J.: Field season 2019 East GReenland Ice core Project (EGRIP) 2015-2020: Third year of EGRIP deep drilling, https://eastgrip.nbi.ku.dk/documentation/2019/EGRIP2019FieldPlan_1stVersion.pdf, 2019.

Davies, S. M.: Cryptotephras: the revolution in correlation and precision dating, Journal of Quaternary Science, 30, 114–130, https://doi.org/10.1002/jqs.2766, https://onlinelibrary.wiley.com/doi/abs/10.1002/jqs.2766, 2015.

Eisen, O., Wilhelms, F., Steinhage, D., and Schwander, J.: Improved method to determine radio-echo sounding reflector depths from ice-core profiles of permittivity and conductivity, Journal of Glaciology, 52, 299–310, https://doi.org/10.3189/172756506781828674, 2006.

Gfeller, G., Fischer, H., Bigler, M., Schüpbach, S., Leuenberger, D., and Mini, O.: Representativeness and seasonality of major ion records derived from NEEM firn cores, The Cryosphere, 8, 1855–1870, https://doi.org/10.5194/tc-8-1855-2014, https://www.the-cryosphere.net/8/1855/2014/, 2014.

Hammer, C. U.: Acidity of Polar Ice Cores in Relation to Absolute Dating, Past Volcanism, and Radio–Echoes, Journal of Glaciology, 25, 359–372, https://doi.org/10.3189/S0022143000015227, 1980.

Hayward, C.: High spatial resolution electron probe microanalysis of tephras and melt inclusions without beam-induced chemical modification, The Holocene, 22, 119–125, https://doi.org/10.1177/0959683611409777, https://doi.org/10.1177/0959683611409777, 2012.

Jensen, B. J. L., Beaudoin, A. B., Clynne, M. A., Harvey, J., and Vallance, J. W.: A re-examination of the three most prominent Holocene tephra deposits in western Canada: Bridge River, Mount St. Helens Yn and Mazama, Quaternary International, 500, 83 – 95, https://doi.org/https://doi.org/10.1016/j.quaint.2019.03.017, http://www.sciencedirect.com/science/article/pii/S1040618218311911, 2019.

Joughin, I., Smith, B. E., Howat, I. M., Scambos, T., and Moon, T.: Greenland flow variability from ice-sheet-wide velocity mapping, Journal of Glaciology, 56, 415–430, https://doi.org/10.3189/002214310792447734, 2010.

Joughin, I., Smith, B. E., and Howat, I. M.: A complete map of Greenland ice velocity derived from satellite data collected over 20 years, Journal of Glaciology, 64, 1–11, https://doi.org/10.1017/jog.2017.73, 2018.

Mojtabavi, S., Wilhelms, F., Franke, S., Jansen, D., Steinhage, D., Dahl-Jensen, D., and Eisen, O.: Deep insights to the Greenland ice sheet by linking multichannel ultra-wide-band radar surveys to the latest deep ice cores by synthetic radar modelling. (manuscript in preparation), 2019.

Moore, J. and Paren, J.: A new technique for dielectric logging of Antarctic ice cores, Journal de Physique Colloques, 48, C1–155–C1–160, https://doi.org/10.1051/jphyscol:1987123, https://hal.archives-ouvertes.fr/jpa-00226268, 1987.

Moore, J. C., Wolff, E. W., Clausen, H. B., and Hammer, C. U.: The chemical basis for the electrical stratigraphy of ice, Journal of Geophys-
315   ical Research: Solid Earth, 97, 1887–1896, https://doi.org/10.1029/91JB02750, https://agupubs.onlinelibrary.wiley.com/doi/abs/10.1029/
91JB02750, 1992.

Moore, J. C., Wolff, E. W., Clausen, H. B., Hammer, C. U., Legrand, M. R., and Fuhrer, K.: Electrical response of the Summit-Greenland ice
core to ammonium, sulphuric acid, and hydrochloric acid, grl, 21, 565–568, https://doi.org/10.1029/94GL00542, 1994.

Mortensen, A. K., Bigler, M., Grönvold, K., Steffensen, J. P., and Johnsen, S. J.: Volcanic ash layers from the Last Glacial Termination in the
320   NGRIP ice core, Journal of Quaternary Science, 20, 209–219, https://doi.org/10.1002/jqs.908, https://onlinelibrary.wiley.com/doi/abs/10.
1002/jqs.908, 2005.

Perkins, M. E., Nash, W. P., Brown, F. H., and Fleck, R. J.: Fallout tuffs of Trapper Creek, Idaho—A record of Miocene explosive volcanism
in the Snake River Plain volcanic province, Bulletin of the Geological Society of America, 107, 1484–1506, https://doi.org/10.1130/0016-
7606(1995)107<1484:FTOTCI>2.3.CO;2, 1995.

325   Perkins, M. E., Brown, F. H., Nash, W. P., Williams, S. K., and McIntosh, W.: Sequence, age, and source of silicic fallout tuffs in mid-
dle to late Miocene basins of the northern Basin and Range province, Bulletin of the Geological Society of America, 110, 344–360,
https://doi.org/10.1130/0016-7606(1998)110<0344:SAASOS>2.3.CO;2, 1998.

Rasmussen, S. O., Andersen, K. K., Svensson, A. M., Steffensen, J. P., Vinther, B. M., Clausen, H. B., Siggaard-Andersen, M.-L.,
Johnsen, S. J., Larsen, L. B., Dahl-Jensen, D., Bigler, M., Röthlisberger, R., Fischer, H., Goto-Azuma, K., Hansson, M. E., and
330   Ruth, U.: A new Greenland ice core chronology for the last glacial termination, Journal of Geophysical Research: Atmospheres, 111,
https://doi.org/10.1029/2005JD006079, https://agupubs.onlinelibrary.wiley.com/doi/abs/10.1029/2005JD006079, 2006.

Rasmussen, S. O., Abbott, P. M., Blunier, T., Bourne, A. J., Brook, E., Buchardt, S. L., Buizert, C., Chappellaz, J., Clausen, H. B., Cook, E.,
Dahl-Jensen, D., Davies, S. M., Guillevic, M., Kipfstuhl, S., Laepple, T., Seierstad, I. K., Severinghaus, J. P., Steffensen, J. P., Stowasser,
C., Svensson, A., Vallelonga, P., Vinther, B. M., Wilhelms, F., and Winstrup, M.: A first chronology for the North Greenland Eemian Ice
335   Drilling (NEEM) ice core, Climate of the Past, 9, 2713–2730, https://doi.org/10.5194/cp-9-2713-2013, https://www.clim-past.net/9/2713/
2013/, 2013.

Ruth, U., Wagenbach, D., Steffensen, J. P., and Bigler, M.: Continuous record of microparticle concentration and size distribution
in the central Greenland NGRIP ice core during the last glacial period, Journal of Geophysical Research: Atmospheres, 108,
https://doi.org/10.1029/2002JD002376, https://agupubs.onlinelibrary.wiley.com/doi/abs/10.1029/2002JD002376, 2003.

340   Seierstad, I. K., Abbott, P. M., Bigler, M., Blunier, T., Bourne, A. J., Brook, E., Buchardt, S. L., Buizert, C., Clausen, H. B.,
Cook, E., Dahl-Jensen, D., Davies, S. M., Guillevic, M., Johnsen, S. J., Pedersen, D. S., Popp, T. J., Rasmussen, S. O., Sever-
inghaus, J. P., Svensson, A., and Vinther, B. M.: Consistently dated records from the Greenland GRIP, GISP2 and NGRIP ice
cores for the past 104 ka reveal regional millennial-scale δ18O gradients with possible Heinrich event imprint, Quaternary Science
Reviews, 106, 29 – 46, https://doi.org/https://doi.org/10.1016/j.quascirev.2014.10.032, http://www.sciencedirect.com/science/article/pii/
345   S027737911400434X, 2014.

Svensson, A., Andersen, K. K., Bigler, M., Clausen, H. B., Dahl-Jensen, D., Davies, S. M., Johnsen, S. J., Muscheler, R., Rasmussen,
S. O., Röthlisberger, R., Steffensen, J. P., and Vinther, B. M.: The Greenland Ice Core Chronology 2005, 15–42ka. Part 2: comparison to
other records, Quaternary Science Reviews, 25, 3258 – 3267, https://doi.org/https://doi.org/10.1016/j.quascirev.2006.08.003, http://www.
sciencedirect.com/science/article/pii/S0277379106002599, 2006.

350   Svensson, A., Andersen, K. K., Bigler, M., Clausen, H. B., Dahl-Jensen, D., Davies, S. M., Johnsen, S. J., Muscheler, R., Parrenin, F.,
         Rasmussen, S. O., Röthlisberger, R., Seierstad, I., Steffensen, J. P., and Vinther, B. M.: A 60 000 year Greenland stratigraphic ice core
         chronology, Climate of the Past, 4, 47–57, https://doi.org/10.5194/cp-4-47-2008, https://www.clim-past.net/4/47/2008/, 2008.

      Vallelonga, P., Christianson, K., Alley, R. B., Anandakrishnan, S., Christian, J. E. M., Dahl-Jensen, D., Gkinis, V., Holme, C., Jacobel,
         R. W., Karlsson, N. B., Keisling, B. A., Kipfstuhl, S., Kjær, H. A., Kristensen, M. E. L., Muto, A., Peters, L. E., Popp, T., Riverman,
355   K. L., Svensson, A. M., Tibuleac, C., Vinther, B. M., Weng, Y., and Winstrup, M.: Initial results from geophysical surveys and shallow
         coring of the Northeast Greenland Ice Stream (NEGIS), The Cryosphere, 8, 1275–1287, https://doi.org/10.5194/tc-8-1275-2014, https:
         //www.the-cryosphere.net/8/1275/2014/, 2014.

      Vinther, B. M., Clausen, H. B., Johnsen, S. J., Rasmussen, S. O., Andersen, K. K., Buchardt, S. L., Dahl-Jensen, D., Seierstad, I. K.,
         Siggaard-Andersen, M.-L., Steffensen, J. P., Svensson, A., Olsen, J., and Heinemeier, J.: A synchronized dating of three Greenland
360   ice cores throughout the Holocene, Journal of Geophysical Research: Atmospheres, 111, https://doi.org/10.1029/2005JD006921, https:
         //agupubs.onlinelibrary.wiley.com/doi/abs/10.1029/2005JD006921, 2006.

      Wilhelms, F.: Leitfähigkeits- und Dichtemessung an Eisbohrkernen(Measuring the conductivity and density of ice cores), Berichte zur Po-
         larforschung, 1996.

      Wilhelms, F.: Messung dielektrischer Eigenschaften polarer Eiskerne (Measuring the Dielectric Properties of Polar Ice Cores), Berichte zur
365   Polarforschung = Reports on Polar Research, 367, https://doi.org/10.2312/BzP_0367_2000, 2000.

      Wilhelms, F.: Explaining the dielectric properties of firn as a density-and-conductivity mixed permittivity (DECOMP), Geophysical Research
         Letters, 32, https://doi.org/10.1029/2005GL022808, https://agupubs.onlinelibrary.wiley.com/doi/abs/10.1029/2005GL022808, 2005.

      Wilhelms, F., Kipfstuhl, J., Miller, H., Heinloth, K., and Firestone, J.: Precise dielectric profiling of ice cores: a new device with improved
         guarding and its theory, Journal of Glaciology, 44, 171–174, https://doi.org/10.3189/S002214300000246X, 1998.

370   Winski, D. A., Fudge, T. J., Ferris, D. G., Osterberg, E. C., Fegyveresi, J. M., Cole-Dai, J., Thundercloud, Z., Cox, T. S., Kreutz, K. J.,
         Ortman, N., Buizert, C., Epifanio, J., Brook, E. J., Beaudette, R., Severinghaus, J., Sowers, T., Steig, E. J., Kahle, E. C., Jones, T. R.,
         Morris, V., Aydin, M., Nicewonger, M. R., Casey, K. A., Alley, R. B., Waddington, E. D., Iverson, N. A., Dunbar, N. W., Bay, R. C.,
         Souney, J. M., Sigl, M., and McConnell, J. R.: The SP19 chronology for the South Pole Ice Core – Part 1: volcanic matching and annual
         layer counting, Climate of the Past, 15, 1793–1808, https://doi.org/10.5194/cp-15-1793-2019, https://www.clim-past.net/15/1793/2019/,
375   2019.

      Wolff, E. W., Chappellaz, J., Blunier, T., Rasmussen, S. O., and Svensson, A.: Millennial-scale variability during the last glacial: The ice
         core record, Quaternary Science Reviews, 29, 2828 – 2838, https://doi.org/https://doi.org/10.1016/j.quascirev.2009.10.013, http://www.
         sciencedirect.com/science/article/pii/S0277379109003588, 2010.